Optics Letters

Phase-shifting radial-shearing digital holography with Greek-ladder zone plates

Simin Zhang,[1,2] Junyong Zhang,[1,*] Wei Fan,[1] Shenlei Zhou,[1] and Jianqiang Zhu[1]

[1]Key Laboratory of High Power Laser and Physics, Shanghai Institute of Optics and Fine Mechanics, Chinese Academy of Sciences, Shanghai 201800, China
[2]University of Chinese Academy of Sciences, Beijing 100049, China
*Corresponding author: zhangjy829@siom.ac.cn

Received 10 August 2018; revised 22 October 2018; accepted 23 October 2018; posted 24 October 2018 (Doc. ID 341963); published 12 November 2018

Holography has been widely applied in fields of imaging and measurement, but the optical setup of traditional phase-shifting holography is complicated. Here, a kind of phase-shifting radial-shearing holography with Greek-ladder zone plates is presented, which largely simplifies the optical configuration for holographic recording and enhances the stability of system. A 1951 U.S. Air Force resolution test target is measured by experiment to verify the validity of our proposed method. Benefiting from amplitude-only diffractive lenses and high stability of the common path, the phase-shifting radial-shearing interference with Greek-ladder zone plates has great potential in biological imaging and x-ray holography for the next generation of synchrotron light sources.

https://doi.org/10.1364/OL.43.005575

Holography is a mature three-dimensional imaging technique with high efficiency and high resolution. Due to its capability of recording the amplitude and phase information of object waves, holography has been widely applied in various scopes [1–4]. The concept of holography was first proposed by Gabor in 1948 [5]. However, the hologram contained an authentic image and its twin image that polluted the reconstructed image. To overcome this drawback, Leith and Upatnieks proposed the off-axis holography, but this optical configuration cannot take full advantage of the space-bandwidth product of optical detectors [6]. In 1997, phase-shifting technique was introduced into in-line digital holography to eliminate the twin image and DC term in the optical region without sacrificing the detector's space-bandwidth [7]. In addition, the development of photodetector has transformed interference-pattern recorders from photographic plates applied in traditional holography to detector arrays utilized in digital holography, which greatly boosted the progress of holographic technology [8–11].

Under the circumstances where the light source has extremely short wavelength, such as EUV and soft x-rays, the applicability of devices for phase-shifting holography, such as piezoelectric ceramics transducers (PZTs) [7,12], wave plates [13–15], and liquid crystal retarders, or spatial light modulators (SLMs) [16,17], should be reconsidered. PZTs are mainly utilized in the reflected beam paths. Wave plates are ruled out due to the strong absorption of the material at the short wavelength, nor can SLMs be operated in this band. Though diffractive optical elements (DOEs), such as gratings, show great potential in the short-wavelength range, and have been used in phase-shifting holography [18], the huge difference of intensities between the different diffraction orders of gratings severely degrades the contrast of interference fringes. To overcome the shortcoming of phase-shifting technology in short-wavelength range, especially in soft x-rays, a kind of amplitude-only phase-shifting Greek-ladder lens has been introduced into the in-line holography [19]. Nevertheless, the above optical configuration is in-line by two light paths but not strictly common-path, which also limits its application in x-rays regime. Though coherent diffraction imaging has been widely used in the region of x-rays because of its lens-free optical path, it relies on the time-consuming phase retrieval algorithms [20]. Thanks to the holographic radial shear interferometer with the Gabor zone plate presented in 1974, the promising common-path configuration began to be applied in holography [21]. Based on the radial shear interferometer, two zone plates were proposed to replace the Gabor zone plate to measure the wavefront [22]. However, the Zernike polynomial method can only measure wavefronts consisting of low frequency, and the optical path is still too complex for x-rays regime. In 2007, a kind of phase-shifting interferometry was proposed to reconstruct the object wave in a common-path fluorescent holography by use of beam splitting function of SLMs [23], which brought the hope for the radial shear interferometer to measure objects with fine structures.

Based on previous work [24–27], we propose the phase-shifting radial-shearing holography with Greek-ladder zone plates. An amplitude-only Greek-ladder zone plate is essentially a splitting diffractive lens that can generate two diffraction-limited foci with equal intensity. Here, a group of Greek-ladder zone plates are designed separately and used to generate three pairs of bifocal spots with different phase shifts. We first carried out the numerical simulation and then verified the validity of our proposed method by measuring a 1951 U.S. Air Force

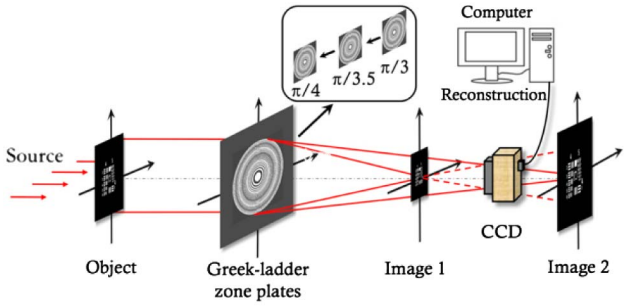

Fig. 1. Principle of the phase-shifting radial-shearing with Greek-ladder zone plates.

resolution test target. The experimental result is in good agreement with the theoretical analysis. The phase-shifting radial-shearing holography with Greek ladder zone plates has many advantages, such as simple operation, strong anti-interference capability, and high sensitivity. Obviously, this method has great potential in observation of transparent biological cell, nondestructive testing of surfaces and high-resolution biological imaging for the next generation of synchrotron radiation and free electron laser in the future.

The principle of the phase-shifting radial-shearing holography with Greek-ladder zone plates is illustrated in Fig. 1. Herein, the Greek-ladder zone plate is a kind of bifocal diffractive lens with equal intensity. It can produce two images with different transverse magnitudes [27]. The laser beam is collimated and expanded before it illuminates the object. The object wave is then split into two parts by the Greek-ladder zone plates. Each zone plate splits the incident light to two converging spherical waves. The one with an invariable phase is referred to as the object wave, while the other with an extra phase shift is the reference wave. Since both waves carry the information of the object, their statuses can exchange. When the three bifocal zone plates are sequentially moved into the light path, three frames of phase-shifting radial-shearing interference patterns will be recorded by a CCD simultaneously.

To obtain the optimal combination of Greek ladders, we first designed an amplitude-only Greek-ladder zone plate working in the soft x-ray region at 2.8 nm wavelength. As shown in Fig. 2(a), it has a diameter of 20 μm with bifocal lengths of 0.6618 and 0.5572 mm. The phase value in the focal spot corresponding to the long focal length is $\pi/4$. In order to verify the validity of the phase-shifting radial-shearing interferometry, the diffracted field is calculated by the Fresnel-Kirchhoff diffraction formula. The intensity and phase distributions are illustrated at the top of Fig. 3. Herein, the phase value in each Airy disk is constant, and the intensity profiles are identical at the same

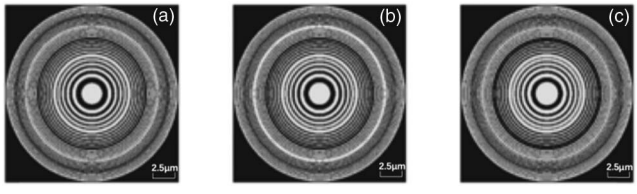

Fig. 2. Structures of three kinds of phase-shifting bifocal zone plates with different phase shifts in focal spots corresponding to their own long focal lengths, (a) $\pi/4$-, (b) $\pi/3.5$-, and (c) $\pi/3$-phase.

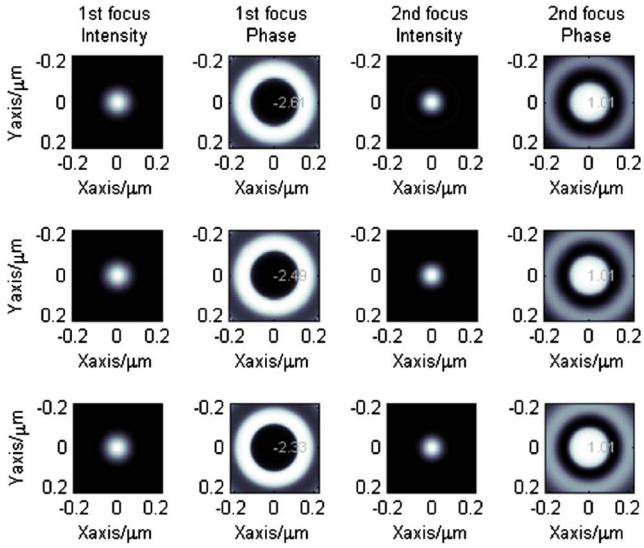

Fig. 3. Intensity and phase distributions of the diffracted field corresponding to (top) Fig. 2(a), (middle) Fig. 2(b), and (bottom) Fig. 2(c).

focal plane. Clearly, the bifocal spots have different phase shifts, each of which can be used to form a frame of radial-shearing interference pattern in the overlapping region of the two beams. Then, with the help of the global optimization algorithm, the fundamental structure of the Greek-ladder zone plate is further optimized. In this case, the focal phase corresponding to the short focal length remains invariable while the focal phase corresponding to the long focal length is variable. Figures 2(b) and 2(c) are the other two kinds of optimized bifocal zone plates with phases of $\pi/3.5$ and $\pi/3$ in the focal spots corresponding to their respective long focal lengths. From the middle and bottom portions of Fig. 3, we know that although the three phase values are the same at the short focal length, the three phase shifts at the long focal length are different. Concretely, the latter ones separately increase $\pi/28$- and $\pi/12$-phase shifts relatively to the fundamental Greek-ladder zone plate. From the viewpoint of imaging, the point spread function decides the imaging properties of a linear imaging system. In other words, the bifocal zone plate can split the object wave into two beams with different curvatures. The beam corresponding to the short focal length is referred to as the object wave, and the other beam corresponding to the long focal length can be considered as the reference waves with different phase shifts. The two beams form a frame of radial-shearing interference pattern on the optical detector. When the former bifocal zone plate is replaced with the two latter bifocal zone plates in sequence, we can get another two frames of radial-shearing interference patterns. The reconstructed wavefront of the object can be easily solved by the following formula [28]:

$$U_o R^*(\theta_1) = I_1(e^{i\theta_2} - e^{i\theta_3}) + I_2(e^{i\theta_3} - e^{i\theta_1}) + I_3(e^{i\theta_1} - e^{i\theta_2}), \quad (1)$$

where I_j is the hologram at the j exposure and θ_j is the phase shift at the j exposure. The field $R(\theta_1)$ corresponds to the reference wave at the first exposure. Note that the constant term has been ignored.

In order to verify the proposed method, a group of Greek ladder zone plates are redesigned to be operated at a wavelength of 632.8 nm based on the above prototype. The zone plates are fabricated on a chrome plate by lithography. Working under the optical wavelength, the zone plates can be replaced with SLMs. Based on the optical configuration in Fig. 1, the wavefront reconstructed by holography is essentially the product of the object wave and the conjugate reference wave. Therefore, only when the optical detector is deviated from the position where the two waves share the same diameter can the crosstalk be greatly reduced. In this case, the intensity of one wavefront is much higher than that of the other wavefront. Obviously, once the optical detector is fixed between the two focal planes of the Greek-ladder zone plate, in the case of coherent light, the shorter the distance between the two focal lengths is, the more significant the crosstalk effect will emerge at the optical detector plane. To make the above analysis more concrete, here is an example presented at a wavelength of 632.8 nm. The test object is a crosshair with half width of 0.33 mm in Fig. 4(a). Three zone plates located in the back focal plane of a 11.26-mm-diameter Fourier lens are all designed to have two focal lengths of 150 and 450 mm, and they provide the object waves with invariable phase and the reference waves with phases of $\pi/4$, $\pi/3.5$, and $\pi/3$ in sequence. The recording distance from the bifocal zone plate to the CCD screen is z_h, the same as the focal length f_o of the Fourier lens. It is clear that the transverse magnification is equal to 1. In order to investigate the crosstalk impact on imaging, the simulation is carried out with $z_h = 225$ mm and $z_h = 440$ mm, respectively. Accordingly, the two Airy radii are approximately 15.42 μm and 30.16 μm. The former recording position is where the two spherical waves coincide perfectly and the contrast of fringes will reach the maximum there whereas the latter is closer to the back focal plane, so the crosstalk should be minimal. The two reconstructed images are shown in Figs. 4(b) and 4(c). It is obvious that Fig. 4(b) has a poorer quality than Fig. 4(c) due to the undesirable crosstalk. The result indicates that the superposition of the two imaging waves degrades the imaging quality considerably.

For fluorescent holography, the best reconstructed image should be attained at $z_h = 225$ mm where the interference contrast is largest [23]. However, in our scenario where the illumination source is coherent light, the reconstructed image manifests a feature of diffraction. This is because the two imaging waves are superimposed on each other, which obscures the reconstructed image [29]. For partial coherent light, the constructed image can be smoothed by the integral of diffraction contributed by different wavelengths; while for coherent light, it becomes vital to find a suitable plane where the information of either image dominates and, at the same time, the

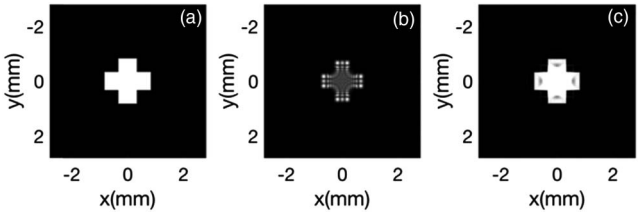

Fig. 4. Simulation of (a) test object and reconstruction at (b) $z_h = 225$ mm and (c) $z_h = 440$ mm.

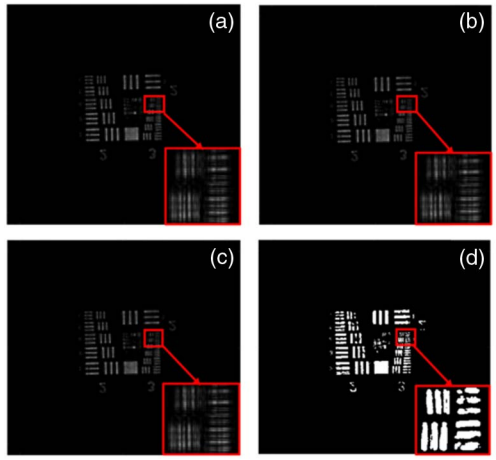

Fig. 5. Experiment results of (a)–(c) radial-shearing interference patterns at $z_h = 440$ mm and (d) reconstructed image.

contrast of the interference fringe is acceptable for the dynamic range of optical detector. Therefore, the recording plane should be near the back focal plane of the bifocal zone plate. In this simulation, it is also proved by the better result at $z_h = 440$ mm, and the four dark arcs in Fig. 4(c) indicate the remnant crosstalk of the two imaging waves.

With the same system parameters in above theoretical analysis, an experiment has also been carried out with a 1951 U. S. Air Force resolution test target. A He–Ne laser of 632.8 nm wavelength and 4 mW output power is used as the source. A CCD with 1392 × 1040 pixels of 6.45 μm × 6.45 μm is utilized as the recorder. The experimental results at $z_h = 440$ mm are shown in Fig. 5. Figures 5(a)–5(c) are the radial-shearing interference patterns recorded by the CCD, and Fig. 5(d) is the reconstructed image. It can be observed from Fig. 5(d) that the group 3 element 6 can be resolved, which indicates that the proposed method is effective.

As known, the resolution target is an amplitude-only object. Relatively, the phase object is more difficult to measure, such as highly transparent cell. Here we take a "peaks" function [30] as a measured phase object, which is representative due to its

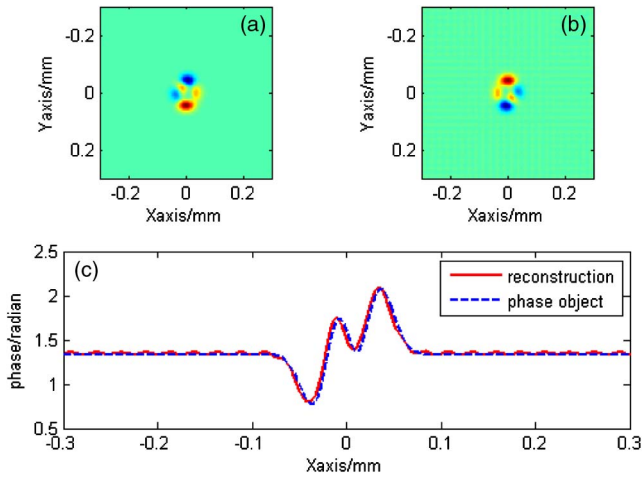

Fig. 6. Simulation results. (a) Phase object; (b) reconstructed image of (a); (c) horizontal phase curves of (a) and (b).

heterogeneous morphology that has features of the overall low phase changes, partially high peak-to-valley values, and the asymmetric structure. Figures 6(a) and 6(b) are respectively the measured phase object and the reconstructed image under the same parameters. Figure 6(c) is the phase curve along the horizontal axis in Figs. 6(a) and 6(b). The full widths of the three peaks are 60.05, 30.03, and 73.70 μm, respectively. Obviously, the phase object is successfully reconstructed, which verifies the validity of our proposed method again.

In conclusion, a kind of phase-shifting radial-shearing holography with Greek-ladder zone plates is analyzed theoretically and demonstrated experimentally. Resembling the beam-splitting function of SLMs, the Greek-ladder zone plates are essentially bifocal diffractive lenses with equal intensity. By reasonable design and optimization, the Greek-ladder zone plates can realize the phase-shifting radial-shearing interferometry. Compared with the traditional in-line holography, the common path of phase-shifting radial-shearing holography is simple and without the troublesome mirrors and combiners. Moreover, due to the amplitude-only diffractive lenses, it will be operative under soft x-rays and applied in high-resolution biological imaging.

Funding. National Natural Science Foundation of China (NSFC) (61775222); Youth Innovation Promotion Association of the Chinese Academy of Sciences (2017292).

REFERENCES

1. T. C. Poon, K. B. Doh, B. W. Schilling, M. H. Wu, K. K. Shinoda, and Y. Suzuki, Opt. Eng. **34**, 1338 (1995).
2. T. Zhang and I. Yamaguchi, Opt. Lett. **23**, 1221 (1998).
3. B. Javidi and E. Tajahuerce, Opt. Lett. **25**, 610 (2000).
4. S. D. Nicola, L. M. P. Ferraro, S. Grilli, R. Meucci, P. K. Buahbassuah, and F. T. Arecchi, Opt. Commun. **281**, 1445 (2008).
5. D. Gabor, Nature **161**, 777 (1948).
6. E. N. Leith and J. Upatnieks, J. Opt. Soc. Am. **52**, 1123 (1962).
7. I. Yamaguchi and T. Zhang, Opt. Lett. **22**, 1268 (1997).
8. J. W. Goodman and R. W. Lawrence, Appl. Phys. Lett. **11**, 77 (1967).
9. S. Grilli, P. Ferraro, S. D. Nicola, A. Finizio, G. Pierattinia, and R. Meucci, Opt. Express **9**, 294 (2001).
10. W. Xu, M. H. Jericho, I. A. Meinertzhagen, and H. J. Kreuzer, Proc. Natl. Acad. Sci. USA **98**, 11301 (2001).
11. I. Yamaguchi, Opt. Lasers Eng. **39**, 411 (2003).
12. I. Yamaguchi, T. Matsumura, and J. Kato, Opt. Lett. **27**, 1108 (2002).
13. T. Kiire, S. Nakadate, and M. Shibuya, Appl. Opt. **47**, 4787 (2008).
14. T. Kiire, S. Nakadate, and M. Shibuya, Appl. Opt. **48**, 1308 (2009).
15. J. Kato, I. Yamaguchi, and T. Matsumura, Opt. Lett. **27**, 1403 (2002).
16. D. W. Griffin, Opt. Lett. **26**, 140 (2001).
17. Y. Awatsuji, M. Sasada, and T. Kubota, Appl. Phys. Lett. **85**, 1069 (2004).
18. J. Li, H. Su, and X. Su, Appl. Opt. **36**, 277 (1997).
19. J. Xie, J. Y. Zhang, Y. L. Zhang, S. L. Zhou, and J. Q. Zhu, Appl. Phys. Lett. **112**, 151906 (2018).
20. J. M. Rodenburg, Adv. Imaging Electron. Phys. **150**, 87 (2008).
21. J. C. Fouere and D. Malacara, Appl. Opt. **13**, 2035 (1974).
22. T. Kohno, D. Matsumoto, T. Yazawa, and Y. Uda, Opt. Eng. **39**, 2696 (2000).
23. B. Katz, J. Rosen, R. Kelner, and G. Brooker, Opt. Express. **20**, 9109 (2012).
24. L. Kipp, M. Skibowski, R. L. Johnson, R. A. R. Berndt, S. Harm, and T. Seemann, Nature **414**, 184 (2001).
25. G. Andersen, Opt. Lett. **30**, 2976 (2005).
26. H. H. Chung, N. M. Bradman, M. R. Davidson, and P. H. Holloway, Opt. Eng. **47**, 118001 (2008).
27. J. Zhang, Opt. Express **23**, 30308 (2015).
28. J. Rosen and G. Brooker, Opt. Lett. **32**, 912 (2007).
29. S. Xu, J. Zhang, S. Zhou, Y. Ma, S. Wang, Y. Zhang, J. Xie, and J. Zhu, Appl. Opt. **57**, 1993 (2018).
30. S. S. Gorthi, G. Rajshekhar, and P. Rastogi, Opt. Eng. **49**, 065802 (2010).